JOURNAL OF PLASTIC SURGERY AND HAND SURGERY
2022, VOL. 56, NO. 5, 310–317
https://doi.org/10.1080/2000656X.2021.1981348

ARTICLE

Innervation of the lumbrical and interosseous muscles in hand: analysis of distribution of nerve fascicles and quantification of their surface projections

Tong Yang[a,b] and Yong-jun Rui[c]

[a]Department of Plastic, Reconstructive and Aesthetic Surgery, The First Hospital Affiliated to Army Medical University, Chongqing, China; [b]Medical College of Soochow University, Suzhou, Jiangsu, China; [c]Department of Hand Surgery, Wuxi No. 9 People's Hospital Affiliated to Soochow University, Wuxi, Jiangsu, China

ABSTRACT

We aimed to determine the surface locations of the nerve fascicles that innervate the lumbricals and interossei, re-examine the branching pattern of the deep branch of the ulnar nerve (dUN), and provide a clear description of their course. Eleven fresh-frozen adult cadaver hands were investigated. Nerve fascicles that innervate the lumbricals, interossei, and surface landmarks including the distal wrist crease and 2–5 proximal finger creases were marked by radio opaque fibers and subjected to X-ray. We analyzed the images and set a quadrant-linked hand surface. Subsequently, we measured the lengths of both axes and the coordinates of the branch locations in the quadrant. The surface locations of branches that innervated the lumbricals and interossei were clearly quantified. The branches of dUN exhibited a 4-group distribution pattern. Novel methods for quantitatively locating the surface anatomy of these branches and demonstration of a 4-group branching pattern of the dUN were established.

Abbreviations: DI1: first dorsal interosseus; DI2: second dorsal interosseus; DI3: third dorsal interosseus; DI4: fourth dorsal interosseus; dUN: deep branch of the ulnar nerve; IMs: interosseous muscles; LMs: lumbrical muscles; L1: first lumbrical; L2: second lumbrical; L3: third lumbrical; L4: fourth lumbrical; MN: median nerve; NFs: nerve fascicles; PI1: first palmar interosseus; PI2: second palmar interosseus; PI3: third palmar interosseus

ARTICLE HISTORY
Received 18 February 2021
Revised 10 August 2021
Accepted 12 September 2021

KEYWORDS
Hand; nerve fascicle; lumbrical muscle; interosseous muscle; surface projection

Introduction

The lumbrical muscles (LMs) and interosseous muscles (IMs) play an essential role in normal hand function [1,2]. These not only contribute to flexion and extension of metacarpophalangeal and interphalangeal joints, respectively, but also maintain the balance of finger movements [1] and broad sweeping movements of the hand [3].

The first and second LMs are normally innervated by the median nerve (MN), while the medial two LMs and all the interossei are innervated by the deep branch of the ulnar nerve (dUN). In recent decades, several studies have revealed detailed information about the innervation of the LMs and IMs. Lauritzen and Szabo [4] described that the first lumbrical (L1) is innervated by the radial digit nerve to the index finger, whereas the second lumbrical (L2) is innervated by the first common palmar digital nerve to the index and middle fingers. In a study by Hur [5], the third lumbrical (L3) was found to be innervated by both the MN and dUN rather than by the dUN alone. Hughes [6] and Atkins [7] depicted the branches of the dUN and the course of these branches to the LMs and IMs. However, many surgeons still have an ambiguous 3-dimensional view of the natural configuration of the innervation of the LMs and IMs. As a result, lesions of these nerve fascicles (NFs) are commonly missed during treatment of palm injuries; in addition, iatrogenic injury to these NFs is likely to occur during dissection of lipomas or ganglions.

Currently, distal nerve transfer is the best technique to minimize time and distance to reinnervate the intrinsic muscles in cases of high median or/and ulnar nerve injury. However, few articles have described motor nerve transfer of LMs and IMs. Besides detailed anatomical information, surface location of NFs that innervate the LMs and IMs are other important factors that determine the precise surgical approach. Knowledge of the surface anatomy of these branches will help surgeons to predict the lesions of the branches during treatment of penetrating or sharp injuries on the palm. However, to the best of our knowledge, no studies have reported the surface location of the branches to the LMs and IMs.

The purpose of this study was to (1) determine the surface location of the NFs that innervate the LMs and IMs; (2) to re-examine the pattern of distribution of the branches of dUN; and (3) to delineate the origin, entrance, and course of these branches. In this paper, we introduce new methods to quantify the locations of the NFs, which are reproducible, accurate, and visualized.

Materials and methods

Dissection

All protocols in this study were approved by the local ethics committee review board. Eleven fresh-frozen Chinese adult cadaver hands were used to investigate the LMs and IMs. Of the 11 hands, 7 were left and 4 were right; 6 were male and 5 were female. The mean age of the cadavers was 72 years (range 32–89 years). No evidence of prior hand injury was observed in any of the

CONTACT Yong-jun Rui yangtongmed@gmail.com Department of Hand Surgery, Wuxi No. 9 People's Hospital, Affiliated to Soochow University, No. 999 Liangxi Road, Wuxi 214062, Jiangsu, China

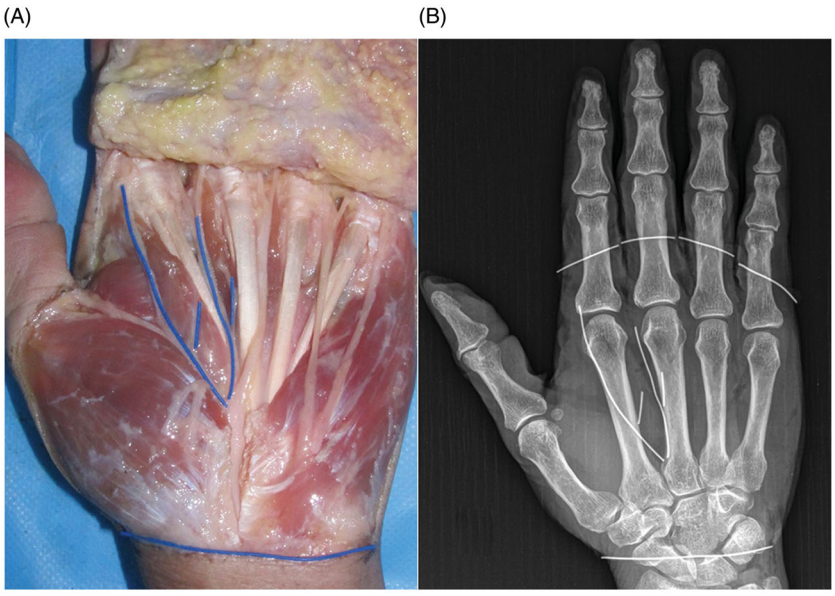

Figure 1. (A) The photograph shows a specimen marked with radio opaque fibers over the nerve fascicles, distal wrist crease and proximal crease of fingers 2–5 (covered by skin). (B) The radiograph shows the marked specimen.

cadavers. All hands were dissected carefully with the aid of a dissecting loop (magnification × 2.5).

There were two layers that required exposure, i.e. a layer superficial to the LMs and a layer deep to the LMs. The skin was incised and reflected distally. After removal of the subcutaneous tissue, palmar aponeurosis, and the arteries, the NFs to the LMs were observed. Then the MN, the tendons of flexor digitorum profundus and flexor digitorum superficialis were cut at the wrist and reflected distally to expose the deep layer. From the origin of the dUN, in the distal and radial direction, the proximal hypothenar muscles were cut and the fat tissue, arteries and adductor pollicis were removed to expose the trunk and branches of the dUN. During dissection, some fascia around the NFs was kept intact to prevent the displacement of fascicles.

Imaging

After completion of dissection of each layer, the NFs, distal wrist crease and 2–5 proximal finger creases were marked by radio opaque fibers (Weian, Xinxiang, China) which were composed of polypropylene and barium sulfate ($BaSO_4$). The fibers were cut to lengths equal to those of the NFs and laid on the surfaces of the corresponding NFs. The fibers are malleable (can be bent into any shape) and radio opaque because of the presence of barium sulfate (Figure 1).

Each layer was X-rayed to obtain a standard anteroposterior view. The wrist was placed in a neutral position, with slight abduction of the thumb and adduction of the 2–5 fingers. All images were uploaded to Picture Archiving and Communication System (Future-med, Beijing, China) for measurement and analysis.

Some surface landmarks were selected to link the surface and the image. These landmarks were the bottom point of the first web space (P), the ulnar border of the palm, the distal wrist crease, and the proximal creases of fingers 2–5. The P is the tip of the acute angle formed by the ulnar border of the thumb and the radial border of the index finger. It also can be easily identified on the image (Figure 2(A)). Because of the thumb, the radial border of the palm is poorly delineated; however, the point P is a helpful reference to identify the radial border of the palm. The ulnar border of the palm is exactly the same as shown in the image. The distal wrist crease and the proximal crease of fingers 2–5 were marked and imaged. The distal wrist crease is the proximal border of the palm, and the proximal crease of fingers 2–5 form the distal border of the palm (Figure 2(A)).

Based on the surface landmarks, a quadrant that covers the whole palm was set in the Picture Archiving and Communication System. First, a line (Y′) was drawn perpendicular to the distal wrist crease, which extended from the distal wrist crease to the middle point of the proximal middle finger crease. It should be noted that the creases exhibit a slight curvature; however, a best fitting straight line which approximates the corresponding crease can be drawn to minimize bias. Then a line segment (Y) that is equal and parallel to the Y′ and passes through the point P was drawn. On the same image, a line (X′) was drawn perpendicular to the Y, extending from the P to the ulnar border of the palm. Finally, a line segment (X) that is equal and parallel to the X′ and superimposed on the distal wrist crease was drawn. Based on the X and Y, the quadrant was completed in which the X and Y were referred to as the *X*-axis and *Y*-axis, respectively (Figure 2(B)). The lengths of the X and Y were equal to the width and length of the palm, respectively.

Measurements and records

All branches were identified with respect to their point of exit from the main nerve and their point of entry into the muscles. The lengths of the branches were measured with the aid of a digital caliper. In the quadrant, the rectangular coordinates (*X*-value, *Y*-value) of the origin and entrance of the branches were measured. For the right hands, the *X* and the *X*-values were presented as absolute values. All the coordinate values were also converted into percentages. The formulas used were: (X-value/$X \times 100\%$; Y-value/$Y \times 100\%$).

Data were collected on a Microsoft Excel spreadsheet and expressed as mean ± standard deviation (SD). The percent values of the coordinates were calculated based on the value of the *X* and *Y* and analyzed statistically according to side and gender using independent-sample *t*-test. A value of $p \leq 0.05$ was considered statistically significant.

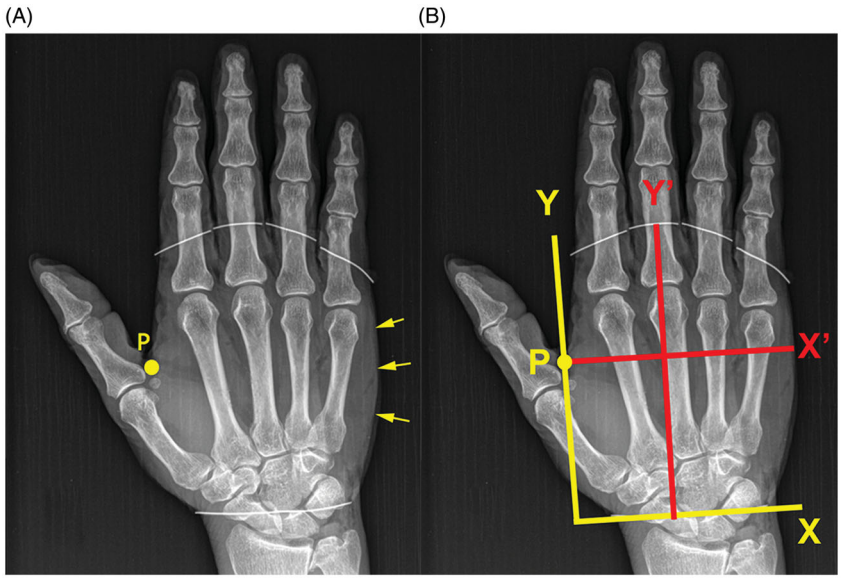

Figure 2. (A) The radiograph shows the surface landmarks, including the bottom point of the first web space (yellow dot with P), the ulnar border of the palm (yellow arrows), the distal wrist crease, and proximal crease of fingers 2–5 depicted by radio opaque lines. (B) The radiograph shows the quadrant set on an image.

Results

Surface locations

The average lengths of *X* and *Y* were 78.27 (SD 8.26) mm and 108.50 (SD7.08) mm, respectively, and no significant differences were found between the left and right hands. Additionally, no significant difference was observed between sexes. Table 1 presents the average length of the branches and the coordinates of their origin and entrance. The surface location and the skeletal relation of each branch are illustrated in Figures 3–5.

Distribution of the dUN

dUN-originating branches were classified into four groups with two variants of innervation. The branches from each group shared a common origin, whereas each variant contained a branch that was not associated with this origin. Table 2 and Figure 6 present detailed information of the branching pattern of dUN.

Origin, entrance, and course of branches innervating the LMs and IMs

In all the specimens, L1 and L2 were innervated by MN, and the fourth lumbrical (L4) and all interossei were innervated by dUN. In 4 of 11 specimens, the L3 was innervated by MN and dUN. The second common palmar digital nerve was the MN branch to the L3 in case of L3 with dual innervation (Figure 7).

L1 was innervated by a branch that separated from the radial digital nerve of the index finger, which traversed along the lateral aspect of the L1. At the middle level of the first metacarpal, it gave a single branch that entered the palmar radial aspect (Figure 8).

L2 was innervated by a branch that separated from the first common palmar digital nerve, which runs toward the cleft between the index and middle fingers. The first common palmar digital nerve traversed above the palmar radial aspect of the L2. At a more distal level than the L1 branch, it gave a single branch to the L2, traversed a longer distance than the L1 branch, and entered the palmar radial aspect of the L2 (Figure 8).

In Group 1, the L4 branch traversed along the ulnar aspect of the third palmar interosseus (PI3). At the proximal level of the deep transverse metacarpal ligament, it divided into two branches; a branch ran straight to supply the fifth metacarpophalangeal joint and the other traversed in the radial direction to supply the L4. In one specimen, the fifth metacarpal was obviously short, and the hypothenar muscles exhibited remarkable atrophy. Due to the variations, the location of the entrance of the branch to the L4 was more proximal and ulnar than the others (Figure 3, data pertaining to its entrance is excluded). The branch to the PI3 accompanied the branch to the L4 for a short distance and entered the palmar aspect of the PI3. After its exit from dUN, the branch to the fourth dorsal interosseus (DI4) traveled deeply to supply the DI4 (Figure 9).

In Group 2, the branch to the L3 exited the dUN and traveled on the surface of the second palmar interosseus (PI2) until its entry into the dorsal ulnar aspect of the L3. In the 4 specimens that exhibited dual innervation, the second common palmar digital nerve traveled over the L3 and produced another branch. The coordinates of the entrances of the two branches to the L3 were exactly equal. The branch to the PI2 accompanied the branch to the L3 for a short distance and entered the palmar aspect of the PI2. After its exit from the dUN, the branch to the third dorsal interosseus (DI3) traveled deeply along the radial side of the PI3 to supply the DI4 (Figure 10).

In Group 3, the branch to the second dorsal interosseus (DI2) traveled radially and distally until its entry into the palmar ulnar aspect of the DI2. The branch to the first palmar interosseus (PI1) traveled more radially than the DI2 branch. It passed across the DI2 and entered the palmar ulnar aspect of the PI1. The branch to the first dorsal interosseus (DI1) proceeded more radially than the PI1 branch. It passed across the DI2 and PI1 and expanded like an "umbrella" and entered the palmar ulnar aspect of the DI1 (Figure 11). In one case, the DI1 branch divided into two branches at the radial side of the PI1, which supplied the DI1.

Discussion

Normal functioning of LMs and IMs is essential for a hand. In high median or/and ulnar nerve lesions, nerve transfer procedure is a

Table 1. Mean (SD) length of the branches and mean (SD) coordinates of the origin and entrance.

	Length (mm)	X-coordinate of origin (%)	Y-coordinate of origin (%)	X-coordinate of entrance (%)	Y-coordinate of entrance (%)
Branch to L1	8.72 (SD 2.12)	29.81 (SD 4.10)	44.67 (SD 4.79)	31.42 (SD 6.61)	53.12 (SD 5.12)
Branch to L2	10.69 (SD 3.40)	39.24 (SD 2.93)	51.02 (SD 4.10)	42.28 (SD 3.49)	60.58 (SD 5.11)
Branch to L3	25.78 (SD 5.27)	58.45 (SD 2.57)	32.23 (SD 1.25)	59.27 (SD 3.17)	55.23 (SD 1.90)
Branch to L4	31.27 (SD 7.13)	63.64 (SD 1.01)	29.67 (SD 2.81)	75.89 (SD 3.33)	57.56 (SD 2.69)
Branch to PI1	13.05 (SD 3.11)	47.83 (SD 5.00)	34.89 (SD 2.25)	36.86 (SD 3.99)	42.99 (SD 3.25)
Branch to PI2	7.05 (SD 2.13)	58.45 (SD 2.57)	32.23 (SD 1.25)	58.89 (SD 2.82)	36.83 (SD 0.84)
Branch to PI3	9.97 (SD 3.75)	63.64 (SD 1.01)	29.67 (SD 2.81)	67.58 (SD 4.13)	37.71 (SD 2.44)
Branch to DI1	20.94 (SD 2.75)	47.83 (SD 5.00)	34.89 (SD 2.25)	19.39 (SD 4.26)	41.88 (SD 2.71)
Branch to DI2	12.28 (SD 2.55)	47.83 (SD 5.00)	34.89 (SD 2.25)	40.52 (SD 3.66)	44.41 (SD 1.73)
Branch to DI3	10.00 (SD 3.14)	55.86 (SD 4.17)	33.29 (SD 1.43)	52.38 (SD 3.42)	38.87 (SD 1.93)
Branch to DI4	9.70 (SD 4.94)	63.46 (SD 1.51)	31.60 (SD 3.50)	63.54 (SD 3.21)	34.15 (SD 2.27)

SD: standard deviation; L1: first lumbrical; L2: second lumbrical; L3: third lumbrical; L4: fourth lumbrical; PI1: first palmar interosseus; PI2: second palmar interosseus; PI3: third palmar interosseus; DI1: first dorsal interosseus; DI2: second dorsal interosseus; DI3: third dorsal interosseus; DI4: fourth dorsal interosseus.

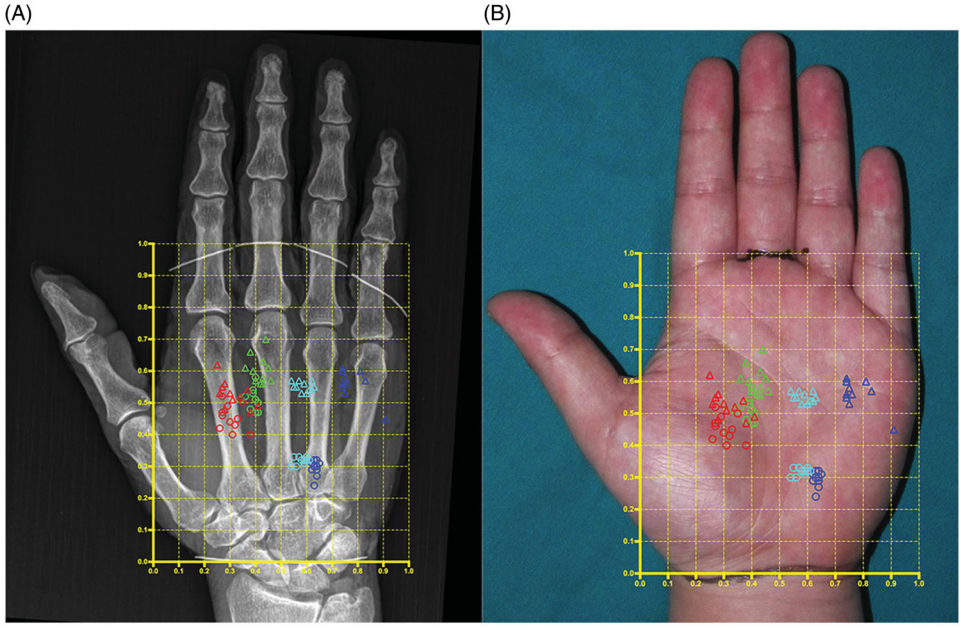

Figure 3. Locations of the origin (circular dots) and entrance (triangular dots) of the branches that innervate the lumbricals are marked on a radiograph (A) and photograph (B). The quadrants and coordinates are expressed as percentage. Red, green, cyan, and blue indicate the branches to the first, second, third, and fourth lumbricals, respectively.

good choice for recovering these functions. However, many surgeons still lack clarity on the natural configuration of the branches that innervate LMs and IMs. Furthermore, no articles have reported the surface anatomy of these branches.

To clearly depict the locations of NFs that innervate the lumbricals and interossei, Gil et al. [8] established a fixed line as a landmark to measure the distances of the origins of the NFs. However, their study provided little information about surface locations and poorly quantified the locations. This study enabled precise visualization of the surface location of the NFs by quantifying their locations. Our methods significantly extend those of Bugbee and Botte [9], who marked palmar skin creases with 25-gauge wires to study the relationship between the palmar skin crease and osseous anatomy. However, considerable inter-individual variability is observed with respect to hand size. To minimize the bias, we converted all coordinate values into percentages based on the lengths of both axes. No differences were observed between sexes and left and right hands, indicating that our methods and results are applicable to healthy individuals.

In the literature, there is little consensus on the dUN branching pattern. Although Linell [10] and Dykes and Terzis [11] could not find evidence of a regular branching pattern of dUN, Homma and Sakai [12] reported that dUN branches exhibit a regular ramification pattern, which corroborate our results. We found that dUN branches to the muscles and joints exhibited a 4-group pattern. Groups 1 and 2 innervated the muscles in the fourth and the third intermetacarpal space, respectively. Group 3 innervated the muscles in the radial two intermetacarpal spaces. In addition, our results extend their findings wherein the branches to the DI4 and DI3 were usually (10/11) and occasionally (3/11) associated with Groups 1 and 2, respectively, indicating that the muscles located in the same ulnar intermetacarpal space may be innervated by branches having a shared origin, rather than distributed innervation.

We confirmed previous findings [4,7] of the origin, entrance and course of the branches that innervate LMs and IMs. We observed dual innervation of L3 in 36.4% of cases (4/11). These innervated L3s were innervated by MN and dUN. These findings corroborate those by Hur [5] but differ from those by Colonna [13]. Hur observed dual innervation of L3 in 64% of cases, while Colonna found no dual innervation of L3. We found no other types of dual innervation of L3, which differs from Hur's results. He reported another dual innervation type wherein the L3 was innervated by MN, dUN, and superficial branch of the ulnar nerve, which is attributable to the larger number of specimens. Colonna [13] observed one case of dual innervation of L2, differing from

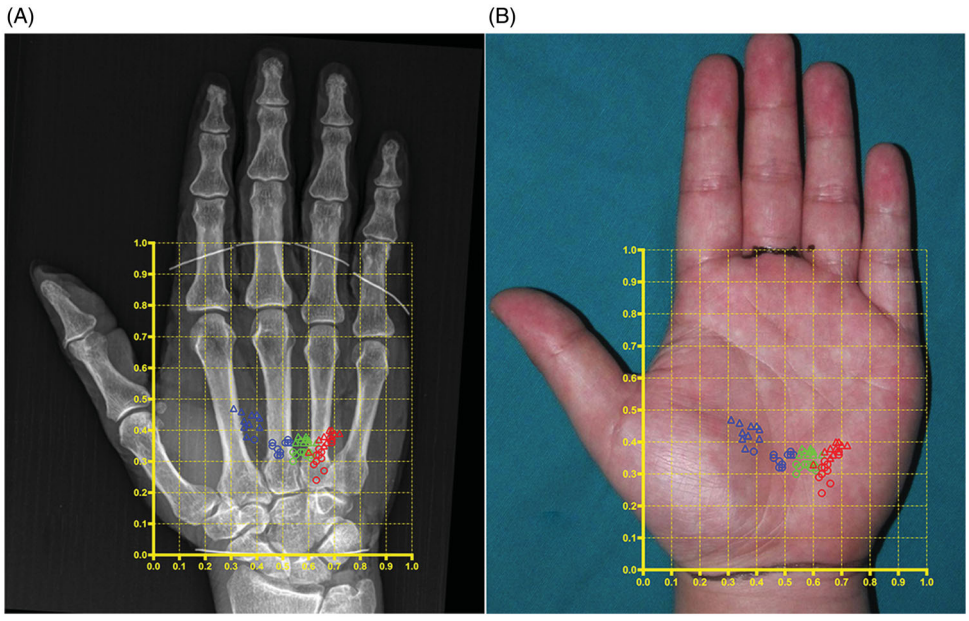

Figure 4. Locations of the origin (circular dot) and entrance (triangular dot) of the branches that innervate the palmar interossei are marked on a radiograph (A) and photograph (B). The quadrants and coordinates are expressed as percentage. Blue, green, and red indicate the branches to the first, second, and third palmar interossei, respectively.

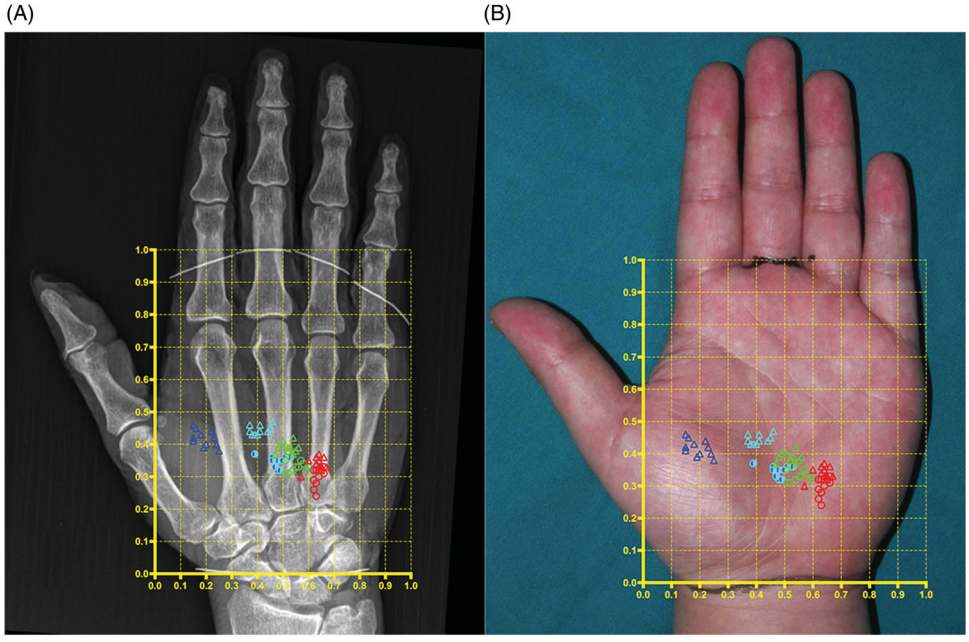

Figure 5. Locations of the origin (circular dot) and entrance (triangular dot) of the branches that innervate the dorsal interossei are marked on a radiograph (A) and photograph (B). The quadrants and coordinates are expressed as percentage. Blue, cyan, green, and red indicate the branches to the first, second, third, and fourth dorsal interossei, respectively. Blue-and-cyan circular dots indicate the shared origin of the branches to the first and second interossei.

Table 2. Branching pattern of the deep branch of the ulnar nerve.

Group	Containing branch/branches innervating to
Group 0	Hypothenar muscles
Group 1	Fourth lumbrical, fourth dorsal interosseus, third palmar interosseus and fifth metacarpophalangeal joint
Ex-Group 1[a]	Fourth dorsal interosseus
Group 2	Third lumbrical, third dorsal interosseus, second palmar interosseus and fourth metacarpophalangeal joint
Ex-Group 2[b]	Third dorsal interosseus
Group 3[c]	Second and first interosseus, first palmar interosseus, and two heads of the adductor pollicis

[a]In 1 of the 11 specimens, the branch to the fourth dorsal interosseus did not share the origin with Group 1 and there was a short distance between the origins of the ex-Group 1 and Group 1.
[b]In 8 of the 11 specimens, the branch to the third dorsal interosseus exhibited the same variant pattern as in ex-Group 1.
[c]In 4 of the 11 specimens, the branch to the DI2 provided a twig to the third metacarpophalangeal joint.

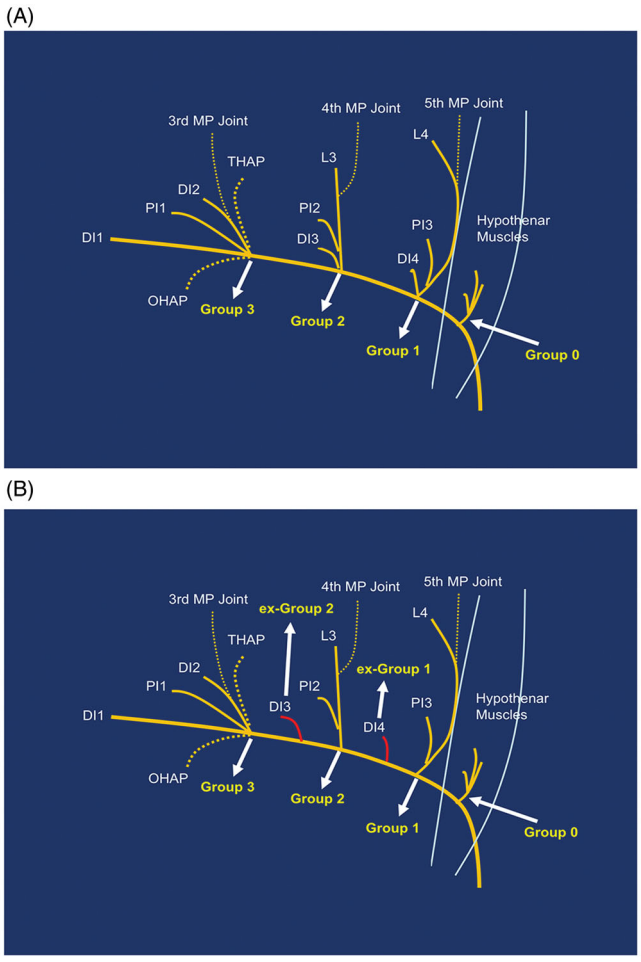

Figure 6. (A) The diagram shows the 4-Group branching pattern of the deep branch of the ulnar nerve. (B) The diagram shows the two variants of innervation, including the ex-Group 1 and ex-Group 2. MP: metacarpophalangeal; THAP: transverse head of adductor pollicis; OHAP: oblique head of adductor pollicis; L3: third lumbrical; L4: fourth lumbrical; PI1: first palmar interosseus; PI2: second palmar interosseus; PI3: third palmar interosseus; DI1: first dorsal interosseus; DI2: second dorsal interosseus; DI3: third dorsal interosseus; DI4: fourth dorsal interosseus.

our results, which showed no dual innervation involving L1, L2, and L4.

Locating the surface anatomy of a target tissue is helpful to clinicians. Wong [14] located facial nerve in order to protect it during parotidectomy. Dupre et al. [15] located supraclavicular brachial plexus for blocking successfully and safely. Wilhelmi et al. [16] used the palmar digital crease and proximal interphalangeal crease to predict the location of the A1 pulley to facilitate minimally invasive release of trigger finger. They [17] also reported that the origin of the thenar branch of the MN can be located on the hand surface with use of the longitudinal line of the third web space and the horizontal cardinal line from the hamate hook to the ulnar border of the thumb as surface landmarks.

Our methods may be applied in various specialities for further studies. Orthopedic surgeons can use these methods to locate the nerves of limbs for surgical safety and to predict fracture-associated nerve injury. Akinleye et al. [18] demonstrated the risk of iatrogenic injuries during percutaneous K-wire insertion for the fifth metacarpal neck fractures, and the risky structure only included tendons and dorsal cutaneous nerves. However, we deem that the branch to the L4 is also at risk (Figure 3). Erhardt and Futterman [19] reported variant innervation patterns of the long

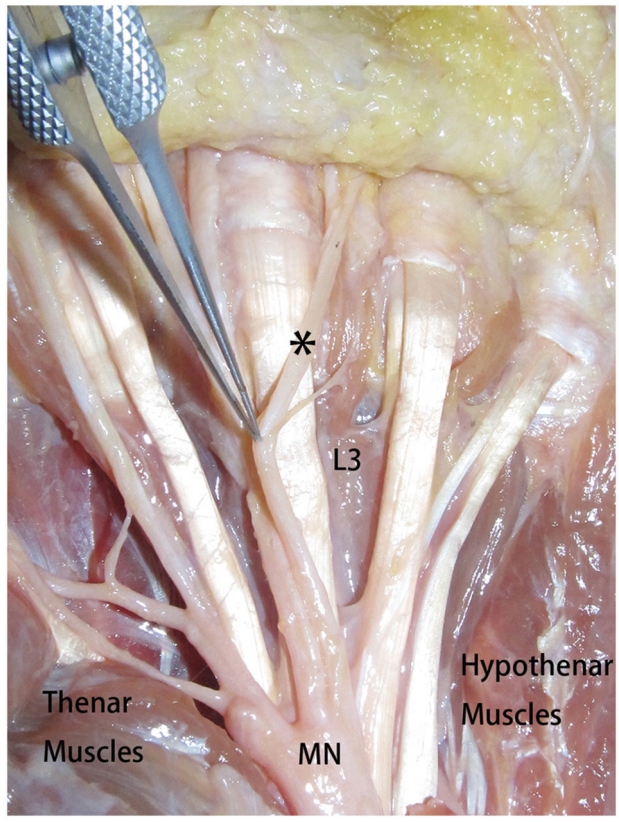

Figure 7. The photograph shows that the second common palmar digital nerve (black asterisk) which originates from the median nerve (MN) sends a branch to innervate the dual innervated L3.

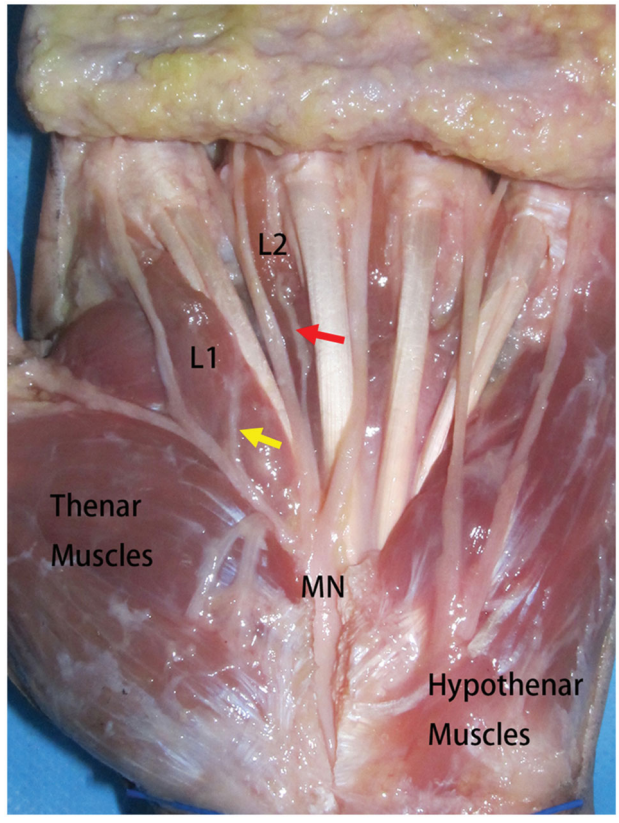

Figure 8. The photograph shows that the radial digital nerve of the index finger sends a branch (yellow arrow) to innervate the first lumbrical (L1) and the first common palmar digital nerve sends a branch (red arrow) to innervate the second lumbrical (L2). MN: median nerve.

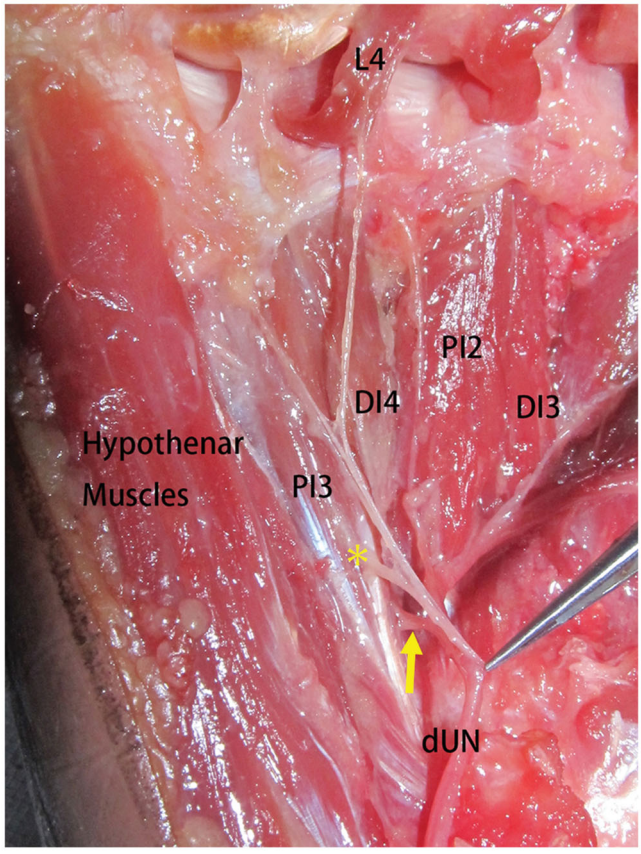

Figure 9. The photograph shows the Group 1. dUN: deep branch of the ulnar nerve; L4: fourth lumbrical; PI2: second palmar interosseus; PI3: third palmar interosseus; DI3: third dorsal interosseus; DI4: fourth dorsal interosseus; yellow arrow: branch innervating the fourth dorsal interosseus; yellow asterisk: branch innervating the third palmar interosseus.

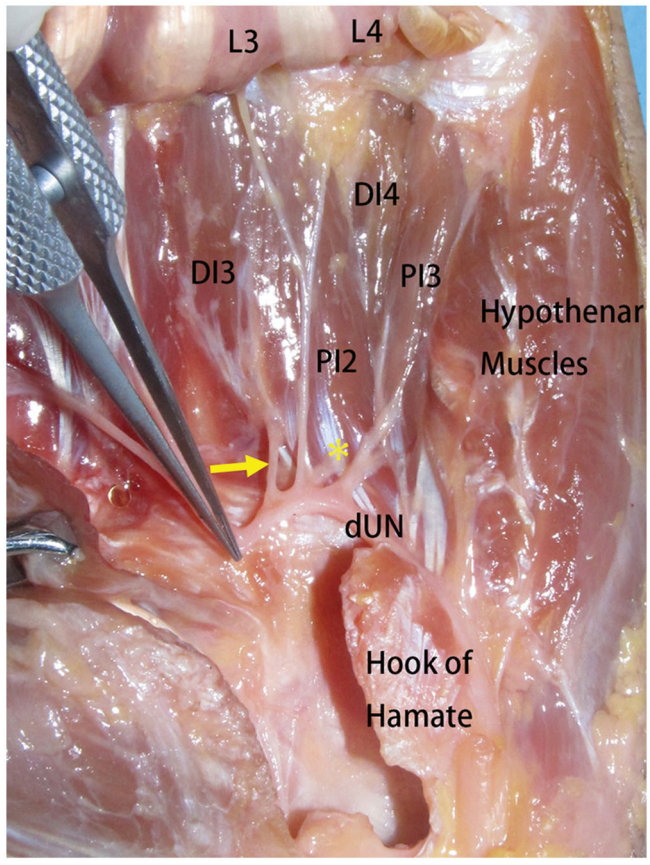

Figure 10. The photograph shows the Group 2. dUN: deep branch of the ulnar nerve; L4: fourth lumbrical; PI2: second palmar interosseus; PI3: third palmar interosseus; DI3: third dorsal interosseus; DI4: fourth dorsal interosseus; yellow arrow: branch innervating the third dorsal interosseus; yellow asterisk: branch innervating the second palmar interosseus.

head of the triceps brachii. Their findings to some extent are still unfamiliar to orthopedic surgeons. Our methods may be further refined to clarify the locations of these variant branches. Furthermore, plastic surgeons can use the methods to design new procedures for nerve transfer. Lee et al. [20] reported the innervation pattern of muscles in the upper extremity to facilitate reconstructive surgery and measured the locations of the NFs using some bony landmarks. Our methods may help formulate the surgical approach for novel nerve transfer procedures. Electromyography examiners can use this method to locate branches to small muscles or muscles with multiple heads for a more precise diagnosis. Surface location knowledge of the entrance of the NFs to the target muscles may facilitate precise penetration of the probe.

Our results quantitatively visualized the locations of the branches innervating LMs and IMs, suggestively solving the diagnosis puzzle in patients with isolated dysfunction of the lumbrical or interosseus resulting from an injury to the palm region. In high median or ulnar nerve lesions, reinnervation of the intrinsic muscles is impossible because of the long distance over which axons regenerate. Nerve transfer may be a potential decision to reconstruct the function of intrinsic muscles because of the shortened distance. Previously, a procedure for transferring the motor branch of the abductor digiti quinti to reinnervate thenar muscles in patients with high MN injuries was reported [21]. The patients involved in this study recovered near 75% of grasp and pinch strength compared with their normal side. Additionally, Bertelli [22] reported a procedure that transferring the branch of the

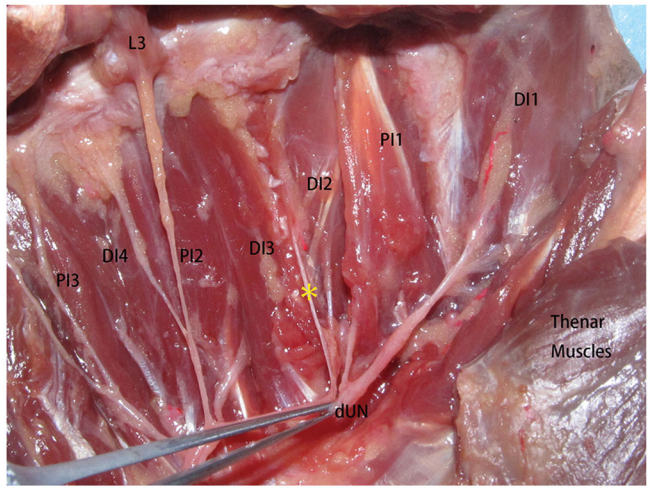

Figure 11. The photograph shows the Group 3. dUN: deep branch of the ulnar nerve; L3: third lumbrical; PI1: first palmar interosseus; PI2: second palmar interosseus; PI3: third palmar interosseus; DI1: first dorsal interosseus; DI2: second dorsal interosseus; DI3: third dorsal interosseus; DI4: fourth dorsal interosseus; yellow asterisk: branch to the third metacarpophalangeal joint.

opponens pollicis to the terminal division of the deep branch of the ulnar nerve for pinch reconstruction. The patients involved in this study had 80–90% improvement in pinch-to-zoom strength. Colonna [23] introduced a novel method for transferring the L1's branch to the distal ulnar nerve motor branch in a cadaveric

study. Our findings may be helpful in designing procedures for transfer of motor branches of LMs and IMs. In our results, the distance between the origin of the branch of the L1 (29.81, 44.67) and the entrance of the branch of the D1 (19.39, 41.88) was short, that can provided support to Colonna's study [23] and broadened Bertelli's study [22].

This study has certain limitations. First, because of a small sample size, some variations of the innervation or findings may not have been observed. Second, setting the *X*- and *Y*-axes is vulnerable to selection bias owing to the crease's natural curvature. Finally, the occupational history or health status of the studied individuals was unknown, which may have influenced our findings.

Overall, our findings enable a clearer view of the natural configuration of the innervation of LMs and IMs, facilitating surgeons to design and perform nerve transfer operations of the hand and safely and precisely tackle such lesions. We also demonstrated a 4-group branching pattern of dUN, extending the current knowledge. Future work should include creation of a 3-dimensional view of these NFs and designing of a surgical approach for their exposure.

Ethical publication statement

Each author certifies that his or her institution approved or waived approval for the human protocol for this investigation and that all investigations were conducted in conformity with ethical principles of research.

Acknowledgments

The authors thank the following individuals for their assistance in various aspects of the project: Yong-qiang Kang, Jun Wang, Jun Gu, Tao-tao Hui, Peng Xu, and Jiong Yu.

Disclosure statement

Each author certifies that he or she has no commercial associations (e.g. consultancies, stock ownership, equity interest, patent/licensing arrangements, etc.) that might pose a conflict of interest in connection with the submitted article.

ORCID

Tong Yang http://orcid.org/0000-0002-6501-6834

References

[1] Liss FE. The interosseous muscles: the foundation of hand function. Hand Clin. 2012;28(1):9–12.
[2] Palti R, Vigler M. Anatomy and function of lumbrical muscles. Hand Clin. 2012;28(1):13–17.
[3] Arnet U, Muzykewicz DA, Fridén J, et al. Intrinsic hand muscle function, Part 1: creating a functional grasp. J Hand Surg Am. 2013;38(11):2093–2099.
[4] Lauritzen RS, Szabo RM, Lauritzen DB. Innervation of the lumbrical muscles. J Hand Surg: Br Eur Vol. 1996;21(1):57–58.
[5] Hur M. Variations of lumbrical muscle innervation patterns in the hand, focusing on the dual innervation of the third lumbrical muscle: lumbrical muscle innervation patterns. Muscle Nerve. 2017;55(2):160–165.
[6] Hughes LA, Clarke HM. Normal arborization of the deep branch of the ulnar nerve into the interossei and lumbricals. J Hand Surg Am. 1995;20(1):10–14.
[7] Atkins SE, Logan B, McGrouther DA. The deep (motor) branch of the ulnar nerve: a detailed examination of its course and the clinical significance of its damage. J Hand Surg Eur Vol. 2009;34(1):47–57.
[8] Gil YC, Shin KJ, Lee SH, et al. Anatomy of the deep branch of the ulnar nerve. J Hand Surg Eur Vol. 2016;41(8):843–847.
[9] Bugbee WD, Botte MJ. Surface anatomy of the hand: the relationships between palmar skin creases and osseous anatomy. Clin Orthop Relat Res. 1993; 296:122–126.
[10] Linell EA. The distribution of nerves in the upper limb, with reference to variabilities and their clinical significance. J Anat. 1921;55(Pt 2–3):79–112.
[11] Dykes RW, Terzis JK. Functional anatomy of the deep motor branch of the ulnar nerve. Clin Orthop Relat Res. 1977; 128:167–179.
[12] Homma T, Sakai T. Ramification pattern of intermetacarpal branches of the deep branch (Ramus profundus) of the ulnar nerve in the human hand. Acta Anat (Basel). 1991;141(2):139–144.
[13] Colonna MR, Piagkou M, Monticelli A, et al. Lumbrical muscles neural branching patterns: a cadaveric study with potential clinical implications. Hand (New York, NY). 2020;00(0):1–9;155894472096388.
[14] Wong DS. Surface landmarks of the facial nerve trunk: a prospective measurement study. ANZ J Surg. 2001;71(12):753–756.
[15] Dupre LJ, Danel V, Legrand JJ, et al. Surface landmarks for supraclavicular block of the brachial plexus. Anesth Analg. 1982;61(1):28–31.
[16] Wilhelmi BJ, Snyder N, Verbesey JE, et al. Trigger finger release with hand surface landmark ratios: an anatomic and clinical study. Plast Reconstr Surg. 2001;108:908–915.
[17] Wilhelmi BJ, Mowlavi A, Neumeister MW, et al. Surface landmarks to locate the thenar branch of the median nerve: an anatomical study. Plast Reconstr Surg. 2003;111(5):1612–1615.
[18] Akinleye SD, Garofolo-Gonzalez G, Culbertson MD, et al. Iatrogenic injuries in percutaneous pinning techniques for fifth metacarpal neck fractures. HAND. 2017;14:386–392. 155894471773185.
[19] Erhardt AJ, Futterman B. Variations in the innervation of the long head of the triceps brachii: a cadaveric investigation. Clin Orthop Relat Res. 2017;475(1):247–250.
[20] Lee EY, Sebastin SJ, Cheah A, et al. Upper extremity innervation patterns and clinical implications for nerve and tendon transfer. Plast Reconstr Surg. 2017;140(6):1209–1219.
[21] Bertelli JA, Soldado F, Rodrígues-Baeza A, et al. Transfer of the motor branch of the abductor digiti quinti for thenar muscle reinnervation in high median nerve injuries. J Hand Surg Am. 2018;43(1):8–15.
[22] Bertelli JA, Soldado F, Rodrígues-Baeza A, et al. Transferring the motor branch of the opponens pollicis to the terminal division of the deep branch of the ulnar nerve for pinch reconstruction. J Hand Surg Am. 2019;44(1):9–17.
[23] Colonna MR, Pino D, Battiston B, et al. Distal nerve transfer from the median nerve lumbrical fibers to the distal ulnar nerve motor branches in the palm: an anatomical cadaveric study. Microsurgery. 2019;39(5):434–440.